On the Accuracy of Scalar Approximation Technique in Optical Fiber Analysis

KATSUMI MORISHITA, MEMBER, IEEE, YASUYUKI KONDOH, AND NOBUAKI KUMAGAI, SENIOR MEMBER, IEEE

Abstract—**The accuracy of the scalar approximation technique in optical fiber analysis is investigated in detail. The scalar approximate solutions are compared numerically with the vector (rigorous) solutions for various linear refractive-index distributions, and several interesting features which are of practical importance are pointed out.**

I. Introduction

SINCE exact theoretical treatment of optical fibers is difficult and laborious, appropriate approximation techniques have been developed. Among them, scalar approximation analysis is one of the most widely used techniques. To the authors' knowledge, however, the accuracy or the precision of scalar approximation method has not yet been discussed in detail. In the present paper, the scalar approximate solutions are compared numerically with the vector (rigorous) solutions for various modes of propagation in the cylindrical fibers of various linear refractive-index distributions, and several interesting features of scalar approximation analysis which are of practical importance are pointed out.

II. Scalar Approximation Analysis

To treat the circular-cylindrical optical fiber by scalar approximation technique, let us use the circular-cylindrical system of coordinates (r,θ,z) whose z-axis coincides with the center axis of the fiber. It is assumed that the permittivity ϵ of the fiber depends only upon the distance r from the center axis, and the permeability is equal to that of vacuum μ_0. Maxwell's equations can then be expressed in the following form in terms of the transverse electric-field component E_t [1].

$$\nabla^2 E_t + (\omega^2\epsilon\mu_0 - \beta^2)E_t + \nabla\left\{\frac{\nabla\epsilon}{\epsilon}\cdot E_t\right\} = 0. \tag{1}$$

Let us introduce further the following three approximation conditions.

i) The fluctuation in the permittivity distribution $\epsilon(r)$ is small enough in comparing with that of the transverse electric-field component E_t

$$\left|\frac{\nabla\epsilon}{\epsilon}\cdot\frac{E_t}{\nabla\cdot E_t}\right| \ll 1. \tag{2}$$

ii) The magnitude of the discontinuity in $\epsilon, \delta\epsilon$, across the discontinuity boundary is sufficiently small so that the following condition is satisfied:

$$\left|\frac{\delta\epsilon}{\epsilon}\frac{E_{\text{dis}}}{E_{\max}}\right| \ll 1 \tag{3}$$

where $E_{\max}$ is the maximum value of the electric field whereas E_{dis} is the value of the electric field at the discontinuity boundary of ϵ.

iii) The variation of the fields in a transverse direction is small enough in comparing with that in the longitudinal direction.

Applying these three approximation conditions into (1), we get the following scalar wave equation:

$$\nabla^2 E_t + (\omega^2\epsilon\mu_0 - \beta^2)E_t = 0. \tag{4}$$

The boundary conditions can be stated, in our case, that both E_t and $\nabla\cdot E_t$ are continuous across the discontinuity boundary.

A transverse Cartesian component of the field is assumed to be expressed in a form

$$E = R(r)\exp[j(\omega t - m\theta - \beta z)] \tag{5}$$

where $R(r)$ is a scalar function of r alone, ω is an angular frequency of sinusoidal time dependence, β is a propagation constant of the guided mode, and m is an integer representing a number of the field variation in the aximuthal direction θ. Substituting (5) into (4), the equation for the scalar function $R(r)$ is derived as follows:

$$\frac{1}{r}\frac{d}{dr}\left(r\frac{dR}{dr}\right) + \left(\omega^2\epsilon\mu_0 - \beta^2 - \frac{m^2}{r^2}\right)R = 0. \tag{6}$$

In the following analysis, the permittivity distributions are regarded approximately as the multilayer structure as shown in Fig. 1. The scalar wave equation in each layer for which the permittivity is given by ϵ_i can be expressed as

$$\frac{1}{r}\frac{d}{dr}\left(r\frac{dR}{dr}\right) + \left(\omega^2\epsilon_i\mu_0 - \beta^2 - \frac{m^2}{r^2}\right)R = 0. \tag{7}$$

The foregoing equation can be solved exactly, and the propagation constant β is determined to be satisfied that R and dR/dr are continuous across the discontinuity boundary of permittivity.

Manuscript received January 29, 1979.
K. Morishita and N. Kumagai are with the Department of Electrical Communication Engineering, Osaka University, Osaka, 565 Japan.
Y. Kondoh is with Japan Broadcasting Corporation.

0018-9480/80/0100-0033$00.75

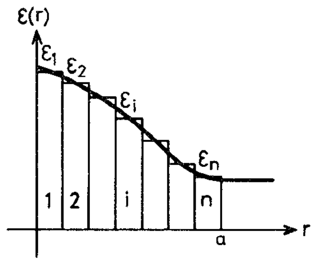

Fig. 1. Multilayer approximation of the permittivity distribution.

For TE mode, the following equations are derived from Maxwell's equations by using $E_z = 0$.

$$\nabla^2 H_t + (\omega^2 \epsilon \mu_0 - \beta^2) H_t = 0 \qquad (8)$$

$$E_t = -\frac{\omega \mu_0}{\beta} i_z \times H_t \qquad (9)$$

$$H_z = \frac{\nabla \cdot H_t}{j\beta}. \qquad (10)$$

Equation (8) must be solved with the boundary conditions that both H_t and $\nabla \cdot H_t$ change continuously. The foregoing differential equation (8) is the same with the scalar approximate wave equation (4), and the boundary conditions stated above are also the same with that in the case of scalar approximation analysis. Therefore, we can get the solution for TE mode by solving the scalar equation without the error due to the scalar approximation.

III. Accuracy of Scalar Approximation Analysis

In this section, the scalar approximation solutions are compared numerically with the results of vector (rigorous) analysis. In order to discuss the effects of a rate of index distribution and an amount of discontinuity of index distribution separately, we shall assume the following linear refractive-index distribution:

$$n(r) = \begin{cases} n_1 \left\{ 1 - 2\Delta\rho\left(\frac{r}{a}\right) \right\}^{1/2}, & a \geqslant r \\ n_1 (1-2\Delta)^{1/2} = n_2, & a < r \end{cases} \qquad (11)$$

where a is the radius of the core, n_1 and n_2 are the refractive indices at the center axis and the cladding of the fiber, respectively, ρ is a factor which characterizes the linear refractive-index distribution profile, and $\Delta \simeq (n_1 - n_2)/n_1$ represents the relative refractive-index difference between the core n_1 (at the center axis) and the cladding n_2. The normalized propagation constant $(\beta - k_0 n_2)/k_0(n_1 - n_2)$ where k_0 is a wave number in free space is calculated numerically by a vector (rigorous) analysis and a scalar (approximation) analysis for various modes of propagation and for various normalized frequency T which is defined by

$$T^2 = 2k_0^2 \int_{n(r) \geqslant n_2} \{ n(r)^2 - n_2^2 \} r \, dr. \qquad (12)$$

In both analyses, the permittivity distribution in a core region is represented approximately by multiple layers of different constant refractive-indices as shown in Fig. 1. So that the matrix method [2] can be employed. In the following numerical evaluation, the core region is divided into fifty layers, and the propagation constants β_{ex} and β_s of various modes are calculated by vector (rigorous) analysis and scalar (approximation) analysis, respectively. The error of the multilayered approximation for both analyses is of the order of 10^{-6} or less in the case of fifty layers division.

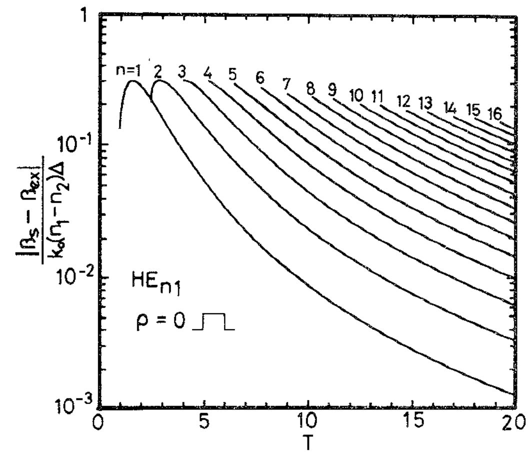

Fig. 2. The error in the propagation constant due to the scalar approximation for HE_{n1} mode. (Step-index fiber.)

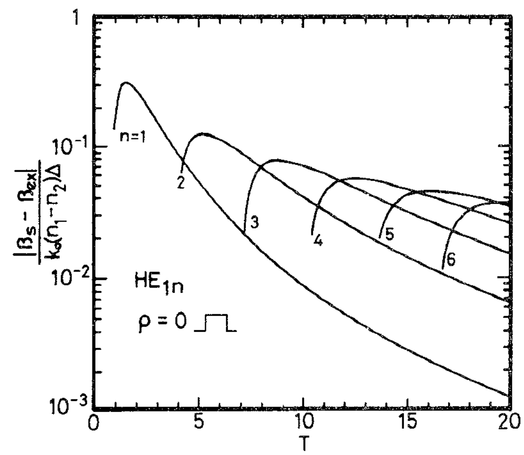

Fig. 3. The error in the propagation constant due to the scalar approximation for HE_{1n} mode. (Step-index fiber.)

One of the interesting features obtained from the numerical calculations is that the error $|\beta_s - \beta_{ex}|/k_0(n_1 - n_2)$ is approximately proportional to the core-cladding refractive-index difference Δ within the range of $\Delta = 0.005 \sim 0.03$.

Figs. 2 through 5 show the error of the normalized propagation constant versus the normalized frequency T for various HE and EH modes in the step-index fiber ($\rho = 0$). The magnitude of the error decreases as the frequency increases and the maximum value of the error decreases a little bit with increasing the mode number. The error becomes very small at the vicinity of the cutoff point except for $HE_{ml}(m \geqslant 2)$ modes, since the cutoff values obtained from the scalar solutions [3] coincide with those obtained from vector solutions [4].

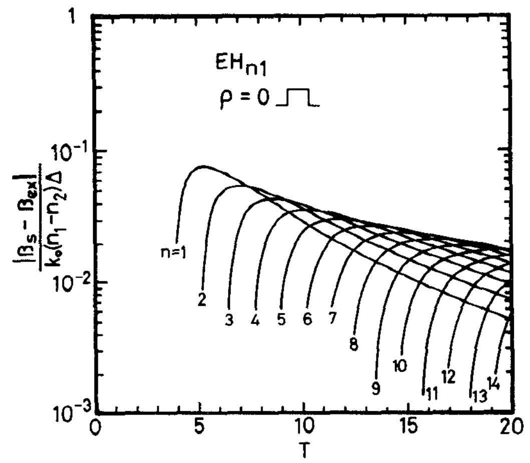

Fig. 4. The error in the propagation constant due to the scalar approximation for EH_{n1} mode. (Step-index fiber.)

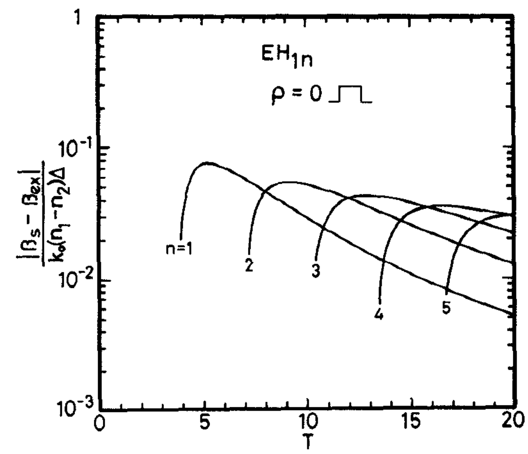

Fig. 5. The error in the propagation constant due to the scalar approximation for EH_{1n} mode. (Step-index fiber.)

Fig. 6 shows the error of the normalized propagation constant versus the normalized frequency for HE_{11} mode in the various linear refractive-index fibers. In the case of the step-index ($\rho=0$) fiber, the error occurs only due to the step discontinuity of the refractive-index distribution. In the case of $\rho=1$, on the other hand, the error comes from the gradient of the refractive-index distribution alone. Therefore, we can see from Fig. 6 that the error due to the step discontinuity decreases more rapidly with increasing the frequency in comparison with the error due to the gradient of the refractive-index distribution. In other words, the most of the error may be caused by the gradient of the refractive-index distribution at the higher frequency.

Fig. 7 shows the error of the normalized propagation constant versus the normalized frequency for TM_{01} mode in the various linear refractive-index fibers. Except the fiber with $\rho=0.5$, the features of the error for TM_{01} mode are similar to that for HE_{11} mode.

Table I shows the numerical values of the error of the normalized propagation constant and the approximation conditions i), ii), and iii) stated in the preceding section. Again we can see from this table that the error due to the discontinuity of the refractive-index distribution ii) de-

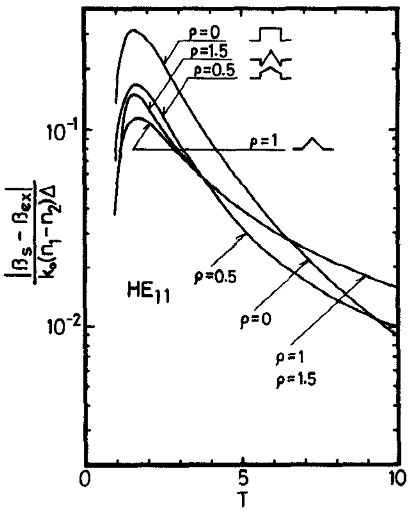

Fig. 6. The error in the propagation constant due to the scalar approximation for HE_{11} mode in the various linear refractive-index fibers.

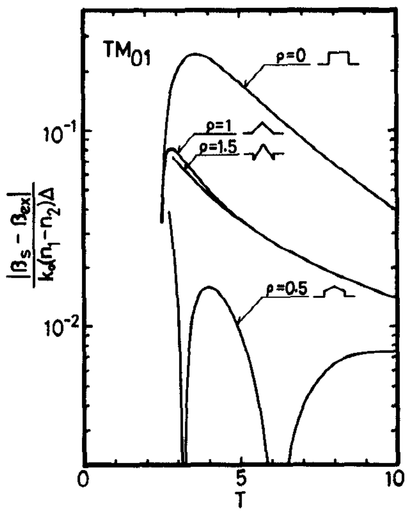

Fig. 7. The error in the propagation constant due to the scalar approximation for TM_{01} mode in the various linear refractive-index fibers.

TABLE I
THE ERROR IN THE PROPAGATION CONSTANT OF LINEAR REFRACTIVE-INDEX FIBERS DUE TO THE SCALAR APPROXIMATION FOR HE_{11} MODE WITH VARIOUS APPROXIMATION CONDITIONS.
$\Delta=0.005,\ u=\sqrt{k_0^2 n_1^2-\beta^2}$

ρ	0		0.5		1		1.5	
T	2	10	2	10	2	10	2	10
ua	1.528	2.185	2.025	5.552	2.987	8.823	4.517	13.24
βa	19.94	99.98	24.41	122.3	34.51	173.0	51.76	259.4
(i) $\frac{2\Delta\rho}{ua}$ $\times 10^{-3}$	0	0	2.469	0.9006	3.348	1.133	3.321	1.133
(ii) $\left\lvert \frac{\delta\varepsilon}{\varepsilon}\frac{E_{dis}}{E_{max}} \right\rvert$ $\times 10^{-4}$	49.6	11.9	20.7	0.444	0	0	2.90	$<10^{-5}$
(iii) $\frac{u}{\beta}$ $\times 10^{-2}$	7.663	2.185	8.296	4.540	8.655	5.100	8.722	5.102
$\frac{\beta_s-\beta_{ex}}{k_c(n_1-n_2)}$ $\times 10^{-4}$	14.1	0.443	7.61	0.496	5.44	0.790	6.40	0.785

creases much more rapidly with increasing the frequency than that caused by the gradient of the refractive-index distribution i).

IV. Conclusion

The accuracy of the scalar approximation technique in optical fiber analysis is discussed numerically in detail for various modes of propagation in the cylindrical fiber of various linear refractive-index distributions. The error due to the scalar approximation depends on the frequency, the refractive-index distribution profile, and the mode of propagation. It is found that, for a given mode and the specific refractive-index distribution, the error increases proportionally with the refractive-index difference Δ between core and cladding. It is shown that the error associated with the gradient of linear refractive-index distribution decreases with frequency faster than that associated with the discontinuity of refractive-index at the core–cladding interface. The accuracy of the scalar approximation analysis for arbitrary refractive-index distributions other than the linear refractive-index distribution may be estimated with the aid of the results shown in this paper.

Acknowledgment

The authors wish to thank Prof. M. Matsuhara of Osaka University for his valuable comments and discussions.

References

[1] C. N. Kurts, "Scalar and vector mode relations in gradient-index light guides," *J. Opt. Soc. Amer.*, vol. 65, no. 11, p. 1235, Nov. 1975.

[2] T. Tanaka and Y. Suematsu, "An exact analysis of cylindrical fiber with index distribution by matrix method and its application to focusing fiber," *Trans. Inst. Electron. Commun. Eng. Jap.*, vol. 59-E, no. 11, p. 1, Nov. 1976.

[3] D. Gloge, "Weakly guiding fibers," *Appl. Opt.*, vol. 10, no. 10, p. 2252, Oct. 1971.

[4] E. Snitzer, "Cylindrical dielectric waveguide mode," *J. Opt. Soc. Amer.*, vol. 51, no. 5, p. 491, May 1961.

Analysis of Open Dielectric Waveguides Using Mode-Matching Technique and Variational Methods

RAJ MITTRA, FELLOW, IEEE, YUN-LI HOU, MEMBER, IEEE, AND VAHRAZ JAMNEJAD

***Abstract*—The mode-matching technique is employed for computing the propagation constants and field distributions of an inverted strip dielectric waveguide. The results derived in this manner are further improved by using variational formulas expressly designed for open dielectric waveguides. Illustrative numerical results are presented and compared with an experimental measurement as well as those based on approximate methods found in the literature.**

Manuscript received March 19, 1979.

R. Mittra is with the Electromagnetics Laboratory, Department of Electrical Engineering, University of Illinois, Urbana-Champaign, IL 61801.

Y. L. Hou is with Litton Systems, Inc., Morris Plains, NJ 07950.

V. Jamnejad is with the Electromagnetics Laboratory, Department of Electrical Engineering, University of Illinois, Urbana-Champaign, IL 61801.

I. Introduction

Recent interest in the 30–300-GHz range, which has remained relatively unexplored hitherto, has led to the investigation of low-loss low-cost dielectric waveguide designs [1]–[4] suitable for integrated circuit applications in this frequency range.

In order to develop reliable designs for uniform dielectric guides as well as for active and passive components constructed from these waveguides, it is extremely important to have the capability of theoretically predicting the performance of these circuit elements and transmission media.